

---

# To Infinity and Beyond: Some ODE and PDE Case Studies

P.G. Kevrekidis<sup>1</sup>, C.I. Siettos<sup>2</sup>, I.G. Kevrekidis<sup>3,\*</sup>,

**1** Department of Mathematics and Statistics, University of Massachusetts Amherst, Amherst, MA 01003-4515, USA

**2** School of Applied Mathematics and Physical Sciences, National Technical University of Athens, GR 15780, Greece

**3** Department of Chemical and Biological Engineering, and Program in Applied and Computational Mathematics, Princeton University, Princeton, NJ 08544 USA; also IAS-TUM, Garching, and Zuse Institute, FU Berlin, Germany. \* correseponding@author.mail

## Abstract

When mathematical/computational problems “reach” infinity, extending analysis and/or numerical computation beyond it becomes a notorious challenge. We suggest that, upon suitable singular transformations (that can in principle be computationally detected on the fly) it becomes possible to “go beyond infinity” to the other side, with the solution becoming again well behaved and the computations continuing normally. In our lumped, Ordinary Differential Equation (ODE) examples this “infinity crossing” can happen instantaneously; at the spatially distributed, Partial Differential Equation (PDE) level the crossing of infinity may even persist for finite time, necessitating the introduction of conceptual (and computational) *buffer zones* in which an appropriate singular transformation is continuously (locally) detected and performed. These observations (and associated tools) could set the stage for a systematic approach to bypassing infinity (and thus going beyond it) in a broader range of evolution equations; they also hold the promise of meaningfully and seamlessly performing the relevant computations. Along the path of our analysis, we present a regularization process via complexification and explore its impact on the dynamics; we also discuss a set of compactification transformations and their intuitive implications..

## Introduction

Studying self-similar solutions that collapse in finite time is a topic of widespread interest in both the mathematical and the physical literature. The contexts range from scaling [1, 2], to focusing in prototypical dispersive equations such as the Korteweg-de Vries (KdV) equation [3] and most notably the nonlinear Schrödinger (NLS) equation [4–6] on the one hand, and from droplets in thin films [7] and flow in porous media [8, 9] to the roughening of crystal surfaces [10] on the other. One may try to avoid collapse (e.g. by imposing space [11–13] or time modulations [14, 15]) or by identifying the higher order effects that preclude collapse in physical experiments [16]. One may alternatively explore what happens to the mathematical, computational (or even physical [17]) setting at, or past, the moment of collapse; see, e.g., the relevant chapter of [6]. With this latter intent, we start here from an array of simple, controllable examples and progressively explore more elaborate ones.

---

Our motivation is simple and, while also physical in part (as in [17], where the impact of collapse on optical filaments is sought), it is chiefly mathematical/computational. As collapse is approached in time, computations naturally break down and so also do, in part, mathematical approaches; there are notable exceptions, e.g. efforts to explore beyond collapse, detailed in the book of [6] for NLS, or in [8,9] for the porous medium problem. This breakdown has motivated extensive efforts to refine computational meshes [18,19] and avoid collapse at the numerical level (possibly transforming into a co-exploding frame, thus factoring out the self-similarity [5,20] as will be discussed further below). Such numerical approaches do not, however, possess the ability to cross infinity, even in a simpler array of examples in which we know by construction, or via analytical arguments, that “life past infinity persists” (i.e., that the solution does not cease to exist and can be continued past a singular point). This is precisely our aim here: we will propose how to numerically go beyond infinity as if it was a regular, rather than a singular point. We construct and apply, on demand, a singular transformation that “absorbs” the singular nature of the dynamics, allowing the solution to re-emerge on the other side of infinity, where the dynamics becomes regular again. A complementary perspective that we explore in this regard is one of compactification transformations which place infinity on equal footing with the rest of the points in, e.g., the ODE orbit.

In ordinary differential equation (ODE) examples, an instantaneous encounter with infinity (crossing or otherwise, as will be discussed below) will be considered in what follows. In partial differential equation (PDE) examples, however, the introduction of physical space leads to multiple possibilities; one is that collapse might only occur at a single physical point/moment in time, with no subsequent continuous “crossing” of infinity. This is the so-called transient blowup in the insightful summary of [21] aiming at the classification (see the discussion of item (5) therein) of post-focusing regimes; we will return to it in our discussion. A number of important examples have this structure, that will not be examined in detail here (although we expect that the techniques proposed below are quite relevant in these cases too). Instead, we will focus on the computationally intriguing case where, upon “touching” infinity at an initial point in space/time, the solution will start gradually crossing; in one dimension this will generically result in two simultaneous crossings that emerge from the original encounter with infinity, and subsequently propagate apart in space/time. This poses computational challenges, as collapse persists in time (there needs to be a singular transformation in some portion(s) of the domain for entire time intervals), and it is also mobile; we need to adaptively follow the region(s) where the singular transformation is detected and accordingly performed as needed. It does not escape us that an additional possibility can be envisaged: finite *spatial* intervals of the solution (possibly multiple ones simultaneously) may become infinite, leading the regular part of the solution to be supported in compact regions, resembling so-called compacton structures originally introduced in [22]. This is referred to as “incomplete blowup” in [21]. Remarkably, complexification of the evolving variable(s) and how this may lead to a *regularization* of the (real) collapsing dynamics naturally emerges as a potential “variant” of collapse. This is, arguably, a topic of interest in its own merit; yet it connects naturally with the overall picture of approaching (and potentially crossing) infinity, and, as such, we will discuss it here.

Our presentation is structured as follows. In Section II, we will briefly outline our ODE examples and their concomitant singular transformations, as well as issues of numerical computation and the notions of compactification, and of regularization via complexification. In section III we will discuss one of the scenarios mentioned above in the case of a 1D PDE. For this purpose, we “engineer” a transformation of a simple, 1D linear reaction-diffusion problem that exhibits the “single initial  $\rightarrow$  multiple

mobile” collapse point(s) scenario; we discuss and illustrate how to address that numerically. We show in this case too how complexification may lead to regularization. We then summarize our findings and present some conclusions and topics for future study. Some relevant auxiliary notions are discussed in the Appendix and the Supporting Information (SI).

## The ODE Context

The standard textbook ODE for collapse in finite time (and its solution by direct integration) reads:

$$\dot{x} = x^2 \Rightarrow x(t) = \frac{1}{t^* - t}. \quad (1)$$

The collapse time  $t^* = 1/x(0)$ , is fully determined by the initial condition, and the textbook presentation usually stops here. A numerical solver would overflow close to (but before reaching)  $t^*$ ; yet we can bypass this infinity by appropriately transforming the dependent variable  $x$  near the singularity. Indeed, the “good” quantity  $y \equiv \frac{1}{x} \equiv x^{-1}$ , satisfies the “good” differential equation  $\frac{dy}{dt} = -1$ ; this equation will help “cross” the infinity (for  $x$ ) by crossing zero and smoothly emerging on the other side (for  $y$ ). Once infinity is crossed, we can revert to integrating the initial (“bad”, but now tame again) equation for  $x$ .

To manifest the feature that infinity crossing should be thought of as being on equal footing with any other point on the rest of this orbit, we introduce a notion of compactification [23]. Reshuffling the (hyperbolic form of the) solution, we have

$$(t^* - t)x = 1 \Rightarrow \left(\frac{t^* - t + x}{2}\right)^2 - \left(\frac{t^* - t - x}{2}\right)^2 = 1. \quad (2)$$

Compactification through the variables  $X$  and  $Y$

$$X = \cos(\theta) = (t^* - t - x)/(t^* - t + x), \quad (3)$$

$$Y = \sin(\theta) = 2/(t^* - t + x). \quad (4)$$

converts this hyperbola to a circle; one can verify that indeed  $-1 \leq X \leq 1$  and  $-1 \leq Y \leq 1$  and also that  $X^2 + Y^2 = 1$ . This puts both relevant infinities

$$(t \rightarrow t^*, x \rightarrow \pm\infty) \Rightarrow (X \rightarrow -1, Y \rightarrow 0^\pm) \quad (5)$$

$$(t \rightarrow \pm\infty, x \rightarrow \pm 0) \Rightarrow (X \rightarrow 1, Y \rightarrow 0^\mp). \quad (6)$$

on equal footing with all other points of the orbit along the circle. The trajectory between the point  $(1, 0)$  (the infinity in  $t$ , the steady state in  $x$ ) and the point  $(-1, 0)$  (the infinity in  $x$ ) can be thought of as reminiscent of a “heteroclinic connection”. Such connections often arise in dynamical systems with symmetries (see e.g. [24, 25]). The compactification also suggests that, provided we utilize “the right variables”, i.e., the right quantities to observe the solution, (e.g., in the form of this circle) we should obtain a consistent, smooth picture (with consistent, smooth numerics). Indeed,  $y(t) = 1/x(t) (= t^* - t)$  is a transformation in itself singular, yet one which converts the “bad” exploding variable  $x(t)$  into a “good” variable  $y(t)$ , satisfying  $\frac{dy}{dt} = -1$  that merely smoothly crosses 0.

The following numerical protocol then naturally circumvents problems associated with infinity in a broad class of ODEs that collapse self-similarly, as power laws of time (or, importantly, as we will see below including in the SI, also *asymptotically* self-similarly):

- Solve the “bad” ODE of Eq. (1) for a while, continuously monitoring, during the integration, its growth towards collapse.
- If/when the approach to collapse is detected, estimate its (asymptotically) self-similar rate (the exponent of the associated power law, here  $-1$ ) and use it to *switch* to a “good” equation for  $y$ , relying on the singular transformation  $y = 1/x$  with this exponent (and on continuity, to obtain appropriate initial data for this good equation).
- Run this “good” equation for  $y$  until 0 for it (or  $\infty$  for the former, “bad” equation) is safely crossed, computationally observing for  $x$  an (asymptotically) self-similar “return” from infinity.
- Finally, transform back to the “bad” equation (no longer that bad, as infinity has been crossed) and march it further forward in time.

This protocol has been carried out in Fig. 1 (see caption), illustrating that the dynamics can cross infinity and computation can be continued for all time, provided that the self-similar approach to infinity is adaptively detected and the associated, and appropriately numerically estimated, singular transformation is used to cross it. Note that the compactification also allows the progression past infinity *in time* too, when now  $y$  crosses zero as time approaches positive infinity and then “returns” from negative infinity.

We can now try to extend/generalize these ideas to other collapse rates (i.e. arbitrary powers/exponents of self-similarity). The collapse of  $\dot{x} = x^3$  whose exact solution is  $x(t) = \frac{1}{\sqrt{t^* - t}}$  is worth examining separately. The relevant singular transformation (here  $y(t) = 1/x^2$ ) will take us to infinity in finite time, but, at first sight, will not cross -  $y(t)$  becomes imaginary beyond  $t^*$ . An appropriate compactification resolves the issue

$$X = \cos(\theta) = (t^* - t - x^2)/(t^* - t + x^2) \quad (7)$$

$$Y = \sin(\theta) = 2/(t^* - t + x^2), \quad (8)$$

leading to perfectly regular dynamics on a circle, so that the singularity is again “bypassed” in the spirit of Fig. 1. Yet an implicit multi-valuedness clearly arises as a crucial issue in selecting useful transformations for such exact solutions; we will return to this important issue below.

For the time being, we argue that one can generalize the above notions for ODEs that asymptotically collapse self-similarly,  $x(t) \sim 1/(t^* - t)^a$ , so as to produce a useful compactification in the form

$$X = \cos(\theta) = ((t^* - t)^a - x)/((t^* - t)^a + x) \quad (9)$$

$$Y = \sin(\theta) = 2/((t^* - t)^a + x). \quad (10)$$

In this form, the dynamics “benignly” travels along the circle. Relevant examples can straightforwardly be extended to, e.g., fractional powers although it is known from standard ODE analysis that issues of uniqueness may arise there that we do not delve into in the present work.

More generally then, the self-similarly collapsing ODE  $\frac{dx}{dt} = \pm x^p$  has the solution  $\pm \frac{1}{1-p} x^{1-p} = t - t^*$  and its scaling in time follows  $x(t) \sim (t^* - t)^{1/(1-p)}$ , with the collapse time once again determined by the initial data. Given a “legacy code” that integrates the ODE  $\dot{x} = F(x)$ , we monitor its growth approaching collapse (i.e., how  $F(x)$  scales as  $x^p$ , or more generally with  $\|x\|$ )<sup>1</sup>. Upon detection of asymptotically

<sup>1</sup>For vector cases, the analogous feature will be to monitor the norm dependence as  $\|x\|^p$ , although we will not explore such a case here.

self-similar collapse, at sufficiently large  $|x|$  (e.g  $10^2$  in the ODE of Fig. 1, or  $10^4$  in the PDEs of the next section) we stop solving the “bad” ODE. We use instead the singular transformation  $y = x^{-p+1}$  (more generally  $y = \int 1/f(x)dx$ ) to solve the “good”  $y(t)$  ODE that crosses 0 rather than infinity. Then, a little beyond the collapse time (beyond infinity for  $x(t)$ , beyond 0 for  $y(t)$ ) we simply revert to the original, “bad” (yet no longer dangerous !) ODE, with continuity furnishing the relevant matching conditions. An illustration of asymptotically self-similar blowups, where different transformations are used to cross two different infinities (the finite-time/infinite value and the infinite-time/finite value ones) is included in the SI.

Examining such infinity crossings as regular, rather than singular points begs an “explanation” for the mechanism of exiting the real axis along  $+\infty$  and then re-emerging on the other side at  $-\infty$  (for  $\frac{dx}{dt} = x^2$ ) or -arguably more remarkably- from  $+i\infty$  back towards the origin in the example involving  $x^3$ ). In the latter case there is an obvious ambiguity: the solution might just as well be chosen to re-emerge from  $-i\infty$ : one can formally, past the collapse, accept  $x(t) = \sqrt{-1/(t-t^*)} = i/\sqrt{t-t^*}$  for  $t > t^*$  or, alternatively,  $x(t) = \sqrt{1/(-(t-t^*))} = -i/\sqrt{t-t^*}$ . This is perhaps a prototypical (and tangible) example of the “phase loss” feature argued in [6, 17].

As a way of shedding further light into these features, we examine the *complexified version* of Eq. (1). The complexified version  $\dot{z} = z^2$  leads to the two-dimensional dynamical system:

$$\dot{x} = x^2 - y^2, \quad \dot{y} = 2xy. \quad (11)$$

The real axis is an invariant subspace, retrieving our real results; yet complexification endows the dynamics with an intriguing “capability”: as Fig. 1 illustrates through the  $(x, y)$  phase plane, collapse *is avoided* in the presence of a minuscule imaginary part. Large “elliptical-looking” trajectories are traced on the phase plane, eventually returning to the neighborhood of the sole fixed point of  $(0, 0)$  –which in the real case one would characterize as semi-stable–. The system of Eq. (11) can be tackled in closed form since the ODE  $\dot{z} = z^2$  yields  $\frac{1}{z} = -t + \frac{1}{z(0)}$ . For  $z = x + iy$  ( $z(0) = x_0 + iy_0$ ) we obtain the explicit orbit formula

$$x(t) = \frac{x_0(x_0^2 + y_0^2) - t(x_0^2 + y_0^2)^2}{(x_0 - t(x_0^2 + y_0^2))^2 + y_0^2} \quad (12)$$

$$y(t) = y_0 \frac{x_0^2 + y_0^2}{(x_0 - t(x_0^2 + y_0^2))^2 + y_0^2}. \quad (13)$$

Eliminating time by dividing the two ODEs within Eq. (11) directly yields an ODE for  $y = y(x)$  (rather than the parametric forms of Eqs. (12)-(13)). From this ODE, one can obtain that the quantity

$$E = \frac{y^2 + x^2}{y} = \frac{y_0^2 + x_0^2}{y_0} \quad (14)$$

is an invariant of the phase plane dynamics, and thus the latter can be written as  $x^2 + (y - R)^2 = R^2$ , where  $R^2 = (x_0^2 + y_0^2)^2 / (4y_0^2)$ . That is, the trajectory evolves along circles of radius  $R$  in the upper (resp. lower) half-plane if  $y_0 > 0$  (resp.  $y_0 < 0$ .) Approaching the axis with  $y_0 \rightarrow 0$ , the curvature of these circles tends to 0 and their radius to  $\infty$  (retrieving the real dynamics as a special case). Fig. 1 through its planar projections illustrates not only the radial projection of the dynamics in the  $x - y$  plane, but the  $x - t$  and  $y - t$  dependencies. Starting with a minuscule imaginary part the real dynamics tends to infinity; yet when the real part gets sufficiently large (somewhat in the spirit of our computations above), the imaginary part “takes over”, grows rapidly, and “chaperons” the real part to the negative side. Once the real part

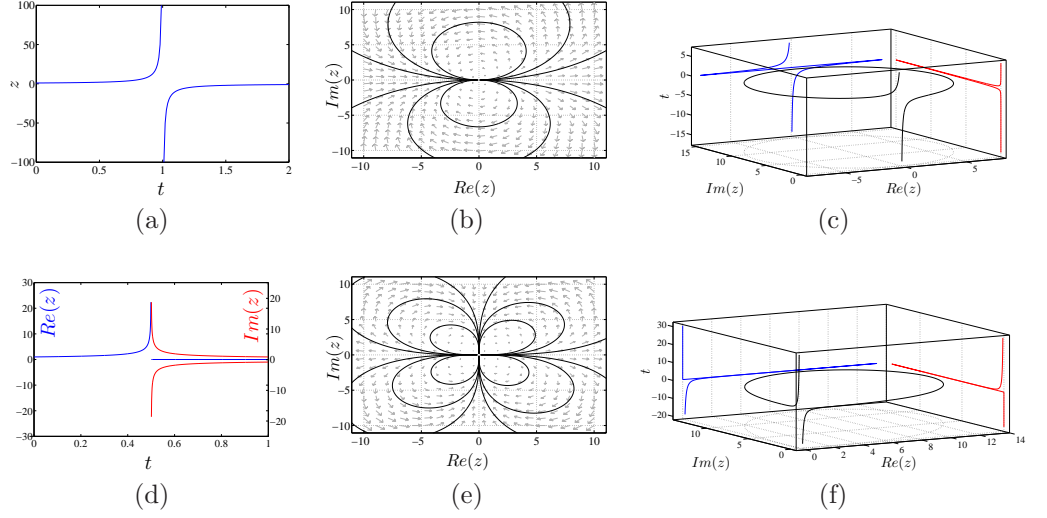


**Figure 1.** (Color online) (a) As discussed in the text, we solve  $\dot{x} = x^2$  until the solution reaches  $x(t) = 100$ , followed by solving Eq. (8) beyond crossing zero to  $y(t) = 0.01$ , and then returning to Eq. (1). Here  $x(0) = 1$ , leading to collapse at  $t^* = 1$ . (b), (c) The complex dynamics of  $\dot{z} = z^2$  as represented by ODEs of Eq. (11). Phase plane analysis (b) and sample trajectory (c). Panel (b) shows that the orbits close (and are, in fact, circles as shown in the text). Panel (c) illustrates the circular nature of the projection in the bottom  $x-y$  plane, as well as the  $x-t$  and  $y-t$  plane projections while following the  $x-y-t$  composite trajectory. (d) In this case, we solve  $\dot{x} = x^3$  until the solution reaches  $x(t) \approx 25$ , followed by solving Eq. (8) beyond crossing zero to  $y(t) = 0.04$ , and then returning to Eq. (1). Here  $x(0) = 1$ , leading to collapse at  $t^* = 0.5$ . (e), (f) The complex dynamics of the two-degree-of-freedom system with  $\dot{z} = z^3$ . An example from the first quadrant of panel (e) is illustrated in more detail in the panel (f), exhibiting how collapse is avoided in this case.

reaches the “opposite” (absolutely equal) negative value, the imaginary part rapidly shrinks and the formerly bad, yet now benign real equation “takes over” again.

We point out here that there is also a canonical way to generalize the compactification of this complex picture to the Riemann sphere through the inverse stereographic projection

$$X = \frac{2x}{x^2 + y^2 + 1} \quad (15)$$

$$Y = \frac{2y}{x^2 + y^2 + 1} \quad (16)$$

$$Z = \frac{x^2 + y^2 - 1}{x^2 + y^2 + 1}. \quad (17)$$

Now the real dynamics become a great geodesic circle, while all other complex plane curves become regular circles on the surface of the sphere. Under this transformation all points with  $x^2 + y^2 \rightarrow \infty$  are identified with  $(0, 0, 1)$ , rationalizing the vanishing time needed to move from one to the other.

For the cubic case  $\dot{z} = z^3$  the two-dimensional dynamical system becomes

$$\dot{x} = x^3 - 3xy^2 \quad (18)$$

$$\dot{y} = 3x^2y - y^3. \quad (19)$$

The corresponding phase portrait is shown in Fig. 1(c), while a typical trajectory is shown in figure Fig. 1(f). Instead of one “leaf” in the upper half plane there are now two leaves, one in each quadrant, see Fig. 1(d); this suggests a natural generalization to  $n - 1$  leaves in each half plane in the case of  $\dot{z} = z^n$ .<sup>2</sup> In the cubic case there is collapse for both positive and for negative initial data, and reentry along either the positive (resp. the negative) imaginary infinity (i.e., from  $+i\infty$ , resp.  $-i\infty$ ) could be chosen (in analogy to the arbitrariness in the phase factor). However, for even infinitesimally small imaginary data, the symmetry is broken, and unique trajectories are selected along each quadrant. A small real part (accompanied by a small imaginary part) as in the bottom right panel of Fig. 1 grows until eventually (when sufficiently large) the imaginary part takes over. The real part then decays rapidly to 0, while the imaginary decays slowly, closing the orbit in the first quadrant; this is again a natural extension of the limiting case of purely real initial data. This complex formulation also allows the quantification (in a vein similar to [26,27]) of how long it takes for initial data, say, on the real axis, to “emerge” on the imaginary axis. In the SI we show that this time tends to 0 for the transitions between  $+\infty$  and  $+i\infty$  for  $\dot{z} = z^3$  (or from  $+\infty$  to  $-\infty$  in  $\dot{z} = z^2$ ).

## A PDE Case

We now turn to a PDE example, illustrating one of the ways that space dependence modifies the crossing of infinity. Motivated by  $\frac{dx}{dt} = \pm x^2$ , where  $x^{-1}$  crosses infinity at a single moment in time, we study the case where infinity is first reached in finite time, and then crossed continuously in time, but (in one spatial dimension) at isolated points in space. The geometry involved is illustrated in the top left panel of Fig. 2, showing a graph of the function  $v(x, t) = x^2 + (0.1 - 0.1t)$ , a parabola shifting its values downwards, at constant speed, but without change of shape. Initially it is everywhere positive; the tip reaches the zero level set at  $t^* = 1$  and then crosses it. The function  $w(x, t) = 1/v(x, t)$  is shown in the top right panel of Fig. 2: it reaches infinity at  $t^* = 1$  and subsequently crosses at two points that move apart as dictated by the motion of the parabola.

We can then agree that the waveform “returns from minus infinity” between these two crossing points as the definition of  $w(x, t)$  formally suggests. Extension to higher-dimensional geometries (e.g. a paraboloid initially touching a plane at a point and then crossing it along a closed curve, such as a circle that “opens up” in time starting at the initial point in two spatial dimensions) can also naturally be envisaged. The key observation is that the evolution of  $w(x, t)$  actually involves a (potentially asymptotically) self-similar collapse near the crossing of infinity. This suggests that, upon detection -on the fly- of such an asymptotically self-similar collapse *and estimation of the associated exponents* (see below) for a “bad”  $w(x, t)$  PDE, a search for a “good observable”  $v(x, t)$  be performed, so that a conceptual and computational program analogous to that of the previous Section on ODEs may be carried through to obtain, and work with, a “good PDE” in the vicinity of the collapse point.

The simple, linear equation

$$u_t = u_{xx} - u \tag{20}$$

provides an “engineered”, yet transparent and analytically tractable illustration of the relevant ideas and hence will be used as our workhorse in what follows. Generic initial

<sup>2</sup>It does not escape us here that a particularly intriguing case in its own right is when  $n$  is rational and perhaps even more so when it is irrational. However, we will restrict our considerations to the simpler integer cases herein, deferring the rest to future work.

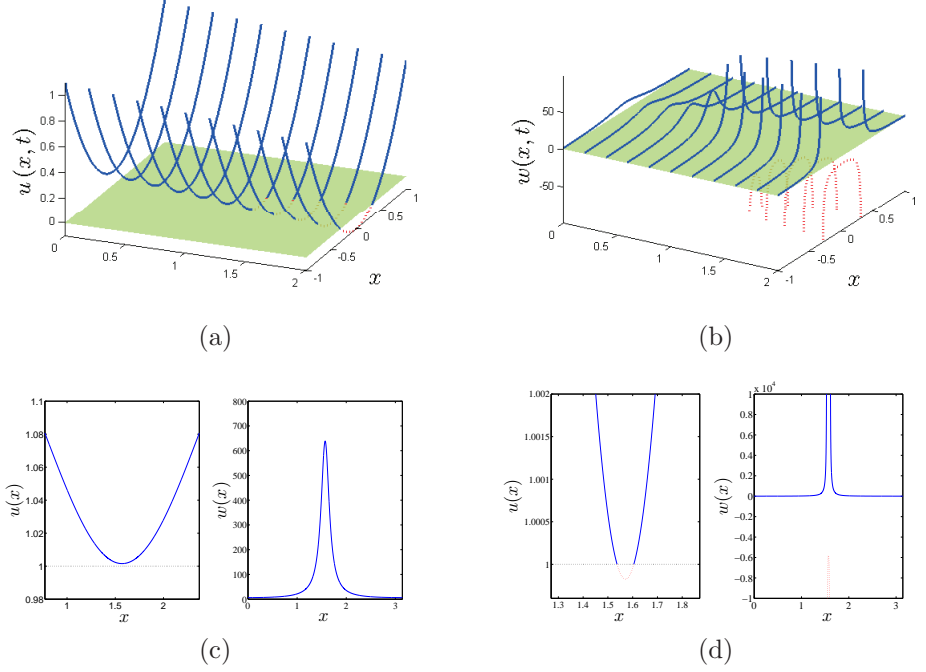


**Figure 2.** (Color online) A geometry for crossing infinity: (a,b) An idealized parabola  $v(x, t)$  (a) shifting at constant speed without change of shape, crossing the 0 level, (b)  $w(x, t) = 1/(v(x, t) - 0)$ . (c,d) Solutions  $u(x, t)$  of Eq. (20) around their crossing of the 1 level, (left panels), and corresponding  $w(x, t) = 1/(u(x, t) - 1)$  (solutions of Eq. (21)) (right panels). (c): just before crossing, and (d): just after crossing infinity.

data in this well-posed, linear model decay and concurrently spread, asymptoting to  $u(x, t) = 0$  at long times. We select an arbitrary level set  $u^* = r > 0$  and a modified variable  $w \equiv \frac{1}{u(x, t) - r}$  to study level set crossings; for initial conditions everywhere above  $r$ , and on its way to zero,  $u(x, t)$  will cross the level set  $r$  so that  $w(x, t)$  will cross *the level set at infinity*.

The “bad” PDE for  $w(x, t)$  reads

$$w_t = w_{xx} - \frac{2}{w} w_x^2 + w + r w^2. \quad (21)$$

An auxiliary tool for the analysis of (asymptotic) self-similar collapse in such equations is the so-called MN-dynamics [20, 28]; a dynamic renormalization scheme rescaling space, time and the amplitude of the solution so that the self-similar solution becomes a steady state in the “co-exploding” frame, i.e., the frame factoring out the symmetry/invariance associated with the (potentially asymptotic) self-similarity. This formulation is presented as a separate, detailed Section in the Appendix for completeness. In that Section, both the general case, and the special example of Eq. (21) are treated. From this formulation we can infer that  $w \sim 1/(t^* - t)$ , which, in turn, suggests the choice of a “good variable” used below.

In our illustrative example we use Neumann BC in  $[0, \pi]$  and initial conditions  $u(x, 0) = a \cos(2x) + c$  (here  $a = 0.4, c = 1.5$ , so that the solution  $u(x, t)$  of Eq. (20) reads:

$$u = 0.4 \exp(-5 * t) \cos(2 * x) + 1.5 \exp(-t), \quad (22)$$



---

and we choose  $r = 1$ . We do not, however, pre-assume such knowledge of  $u(x, t)$  since the equation we have to solve is the “bad” (focusing)  $w(x, t)$  equation, i.e., Eq. (21); our MN framework applied to the focusing of the  $w(x, t)$  evolution then suggests that a good observable is  $v(x, t) \equiv w(x, t)^{-1}$ , a variable that will simply be crossing 0 and thus the “good PDE” would simply be

$$v_t = v_{xx} - v - r \tag{23}$$

The bottom panels of Fig. 2 show representative instances just before and just after the initial encounter of the  $w(x, t)$  profile with infinity in both its “good”  $v(x, t) \equiv (u(x, t) - 1)$  and its “bad”  $w(x, t)$  incarnations, in the spirit of Figures 2a and 2b. The approach to infinity for  $w(x, t)$  is indeed *asymptotically self-similar*, as explained in the Appendix. As we approach the event, an inverted bell-shaped profile comes close to, touches, and then starts crossing through  $r = 1$  in the variable  $u$ , or crossing through 0 in the variable  $v \equiv u - r$ , or equivalently crossing through  $\infty$  in the variable  $w$ .

Recall that our goal is to seamlessly carry out the computation without our numerical code ever realizing that (some part of) the solution is becoming indefinitely large. To achieve this, as the bad PDE solution grows towards infinity, it is adaptively tested, with a user-defined threshold for (local, asymptotic) self-similarity, i.e., for growth according to a (potentially approximate) power law. When this is numerically confirmed, a suitable power law transformation is devised with the numerically estimated similarity exponent; in the above example the detected exponent is  $-1$  and so the transformation is  $v = w^{-1}$ . The easiest way to realize the right observable in this case is to consider uniform initial conditions - then the PDE reduces to an ODE that asymptotically explodes as the  $\dot{w} = w^2$ , suggesting the  $v = w^{-1}$  change of observables.

Importantly, the transformation has to be performed -and the “good” solution sought- over an entire *spatial interval(s)* surrounding the approaching singular point(s). This suggests the following procedure, illustrated schematically in Fig. 3:

- Upon detection of approach to infinity -as the “tip” of the collapsing waveform grows beyond a sufficiently large value- at a given point or points inside the computational domain, we split the domain in 3 regions: (a),(c) regular ones to the left and to the right of the growing tip, where the original “bad” equation for  $w$  is being solved; and (b) a new “singular” one, in the middle, where instead of solving the equation for  $w$ , now the equation for its singularly transformed variant, the “good” equation for  $v = w^{-1}$  is solved instead. The latter transformation is selected to comply with either the self-similar analysis on the theoretical side, or the identified power law of amplitude growth on the numerical side. These equations are linked by continuity of the (transformed) observables at the domain boundaries, and standard domain decomposition numerical techniques are used [29]. The good equation simply crosses zero rather than crossing infinity, as in the ODE case.
- Once zero is crossed, the initial single crossing point in the family of case examples under consideration (in one spatial dimension) “opens up” into *two* infinity crossings (one can visualize two waves that propagate in opposite directions, one to the left and one to the right) - two zero-level-set crossings for the “good” equation. These crossings are quantified, for our example, in Fig. 3. They are bordered by the computed locations of a “high enough” absolute level (here  $10^4$ ) for asymptotic self-similarity.

To deal with the two new crossings computationally over time, the central region is subsequently split into 3 regions. The two outer ones are our “singular

buffers”, surrounding, and in some sense ”masking” the infinity crossings to the left and to the right. But now they are separated by another, inner ”regular” interval, where we can again solve the original ”bad” equation since in here it is again sufficiently far from infinity. Thus, post-collapse, we partition the domain into five regions, three regular ones -the two outer ones, and the innermost, for the ”bad equation”- and then two ”singular buffers” for the transformed ”good” equation, one around the left zero crossing and one around the right zero crossing of  $v$ , that correspond to the two infinity crossings of the bad equation for  $w$ .

A nontrivial aspect of the computation is the ”gluing” between the regular regions and the singular buffers. Our numerical scheme here is a simple one following [29]: for a finite difference discretization in space, (a) an explicit forward Euler time step is performed at the interface points, which provides the interior boundary conditions for the next time step (the next ”computational era”), while (b) an implicit Euler time step is adopted to solve the ”good” and ”bad” PDE within the three (or the five) domains. The scheme can be modified to allow for different space and time steps in the different domains till the next computational era, when the new interface points will be detected, the new ”interior” BCs will be computed, and the new set of BVPs resulting from the implicit timestepping in each domain will be solved. To recap the essence of the algorithm, by solving the ”good” equation inside the buffer regions (and following the motion of the buffers on the fly), we ensure that the numerical simulation is never plagued by the indeterminacy associated with approaching/touching/crossing infinity.

We now explore two more notions that were also examined in the ODE context. The first is compactification: self-similar PDE dynamics, although crossing through infinity, can simply be compactified as evolving over a circle or -better- on a sphere. We perform this step for a general 1D PDE (self-similar) solution of the form –assuming independence from  $\tau$  (see the MN formulation in the Appendix)–

$$u(x, t) = \frac{1}{(t^* - t)^r} f(\xi), \quad (24)$$

where  $\xi$  is a self-similar variable, e.g.  $\xi = x/(t^* - t)^q$ . If the  $\max(f) > 1$ , we can define  $\tilde{f} = f/\max(f)$  and subsequently drop the tilde in Eq. (24) ensuring that  $|f| \leq 1$ . We can then rewrite Eq. (24) as:

$$(t^* - t)^r u = f \Rightarrow ((t^* - t)^r + u)^2 - ((t^* - t)^r - u)^2 = 4f(\xi). \quad (25)$$

Then, upon suitable definition of the variables, we can have  $X = ((t^* - t)^r - u) / ((t^* - t)^r + u)$  and  $Y = 2\sqrt{|f(\xi)|} / ((t^* - t)^r + u)$ , in which case  $X^2 + Y^2 = 1$ . In these variables, at every moment in time the trajectory can be thought of as compactified along a circle. However, as the circle itself represents an invariant shape, in this representation we cannot straightforwardly visualize the trajectory’s dynamics; for this reason, we next compactify the dynamics on a sphere. We define  $g^2 = 1 - f^2$  and we can then write using the above variables  $(gX)^2 + (gY)^2 = g^2 = 1 - f^2$ , which can be reshuffled to read:

$$\left( g \frac{(t^* - t)^r - u}{(t^* - t)^r + u} \right)^2 + \left( g \frac{2\sqrt{f}}{(t^* - t)^r + u} \right)^2 + f^2 = 1. \quad (26)$$

Choosing the three terms of the left hand side of Eq. (26) as

$(X', Y', Z') = (g \frac{(t^* - t)^r - u}{(t^* - t)^r + u}, g \frac{2\sqrt{f}}{(t^* - t)^r + u}, f)$ , we observe that the dynamics can be seen as evolving along the surface of a sphere. This compactification once again underscores the possibility to think of infinity as a regular circle (rather than point, as is the case

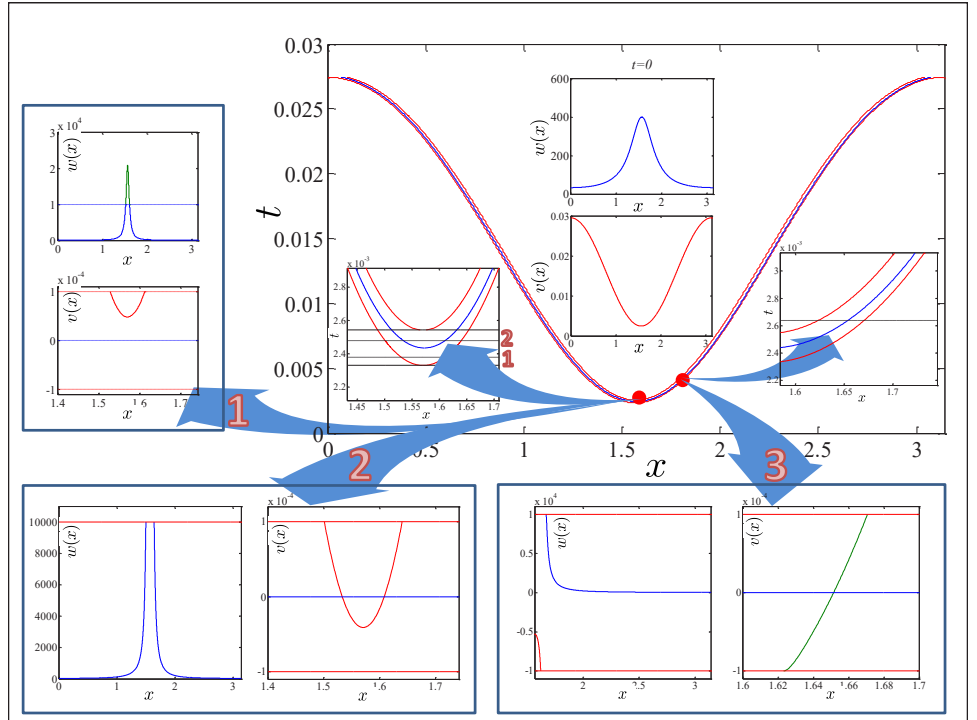


**Figure 3.** Schematic of the computation. The main background figure (top right) shows the locus (in blue) of the points in space-time where  $w$  becomes infinite. The two accompanying red curves define the bands within which we solve the good equation for  $v = 1/w$ . The central top inset is the initial bad equation profile at  $t = 0$ . The central bottom inset is the initial profile of our original motivating linear problem for  $u(x, t)$ . The right inset shows a band crossing infinity in space-time, while the panels (3) show the solution of the good equation (*inside the band*, on the right) and of the bad equation (*outside the band*, on the left). The left inset is more involved since it encompasses two computational “eras”. The first (1), takes place after we have crossed our selected high level (here  $10^4$ ) for  $w$  defining the buffer region boundary, but have not yet crossed infinity; both the bad ( $w$ ) and good ( $v$ ) solutions are shown. The second (2) takes place after  $w$  crossed infinity, but has not (in absolute values) receded below the high level defining the buffer regions. Again both the bad ( $w$ ) and the good ( $v$ ) solutions are shown. The link to a computational movie of this evolution can be found at <https://www.dropbox.com/s/1vag91zuwhjkula/PDEPassInfinity.avi?dl=0>

for ODEs), a level set that is crossed by the PDE solution evolving along the surface of the sphere.

Finally, as in the ODE case, we discuss the possibility of complexifying the model in order to understand, as a limiting case, how infinity is crossed for purely real initial data, while it may be avoided (regularized) upon initialization with complex initial data. Using the complex decomposition for  $w(x) = a(x) + ib(x)$  in Eq. (21), one can obtain the pair of real and rather elaborate looking equations:

$$a_t = a_{xx} - 2a \frac{a_x^2 - b_x^2}{a^2 + b^2} - 4b \frac{a_x b_x}{a^2 + b^2} + a + r(a^2 - b^2) \quad (27)$$

$$b_t = b_{xx} + 2b \frac{a_x^2 - b_x^2}{a^2 + b^2} - 4a \frac{a_x b_x}{a^2 + b^2} + b + 2rab. \quad (28)$$

---

We expect that the presence of an imaginary part in the initial data may avoid collapse in analogy with Figure 1. Given the quadratic nature of the nonlinearity, the quadratic ODE example is especially relevant; we expect here to observe something similar but in a PDE form, having space as an additional variable, over which the profile is distributed (around the crossing “tip”). Again, the tractability of our example allows us, via the solution of Eq. (23), to perform the relevant calculation analytically since at the level of the equation for  $v$  the complex model can be fully solved. Then, assuming  $v = c + id$ , the variable  $w = a + ib = 1/v = 1/(c + id)$  leads to  $a = c/(c^2 + d^2)$  and  $b = -d/(c^2 + d^2)$ , and obtaining  $(c, d)$  explicitly, the same can be done for  $(a, b)$ . This program is carried out in Fig. 4; see also the relevant movie at: <https://www.dropbox.com/s/rxekr7umxa5b3ko/complexdynamics.avi?dl=0>. We reconstruct analytically the spatial profile of the real and imaginary parts of  $w$  at different moments in time provided in the caption. While the profile tends towards collapse in the real part of the variable (and would go all the way to collapse and the dynamics of a Figure like 2 for purely real initial data), the imaginary part, in analogy to the dynamics of Fig. 1, but in a distributed sense around the tip, eventually takes over. As it does so, it forces the solution filament to “turn around on itself” in a spatially distributed generalization of the ODE of Fig. 1. Finally, the solution appears to re-emerge from the other side, practically extinguishing its imaginary part, and having avoided the crossing of infinity. This illustrates how complexification, even in the case of the PDE, results in the avoidance of collapse and the regularization of the model; the collapsing real case is a special limit case of the more general complex one.

## Concluding remarks and future challenges

We attempted to address here a few prototypical cases of a spectrum of problems arising in both ordinary and partial differential equations, so as to deal with the emergence of infinities during the evolution of the relevant models. In a number of cases the model at hand will become physically inaccurate, and will need to be suitably modified as these singular points are approached; if not, our questions may be relevant for the physical realm. In any event, the questions are of particular relevance towards the mathematical analysis and numerical computation of the models at hand. In that light, we argued that it is possible in our context to perform singular transformations on demand, that may sidestep -through the help of a “good equation”- the computational difficulties associated with infinities, rendering them tantamount to the crossing of a regular point such as zero. For ordinary differential equations, once the crossing has transpired, one can safely return to the original “bad” equation and continue the dynamics from there (until possibly a new infinity is approached).

In the case of partial differential equations, the scenario at hand is more complex. There, the solution is distributed in space, and hence we assume and have analyzed the setting where a (generically assumed to be parabolic; see the relevant discussion in the Appendix) tip of a waveform approaches infinity. We have discussed in detail a scenario of initially touching infinity and then crossing it. Suitable computational “buffers” need then to be devised, where the detected singular transformation allows us to locally re-interpret (for computational purposes) the crossing of infinity as the crossing (in a transformed space) of a regular point, such as zero. These buffers need to be in constant and consistent communication, through appropriate continuity conditions, with the rest of the computational domain (the “rest of the world”). Typically, the buffers are defined by the location at which the solution takes on a sufficiently large (absolute) value - say  $10^4$  to the left and right of the growing tip in the pre-crossing regime, or, say,  $10^4$  till  $-10^4$  on the left, and  $-10^4$  till  $10^4$  on the right in the post-crossing regime.

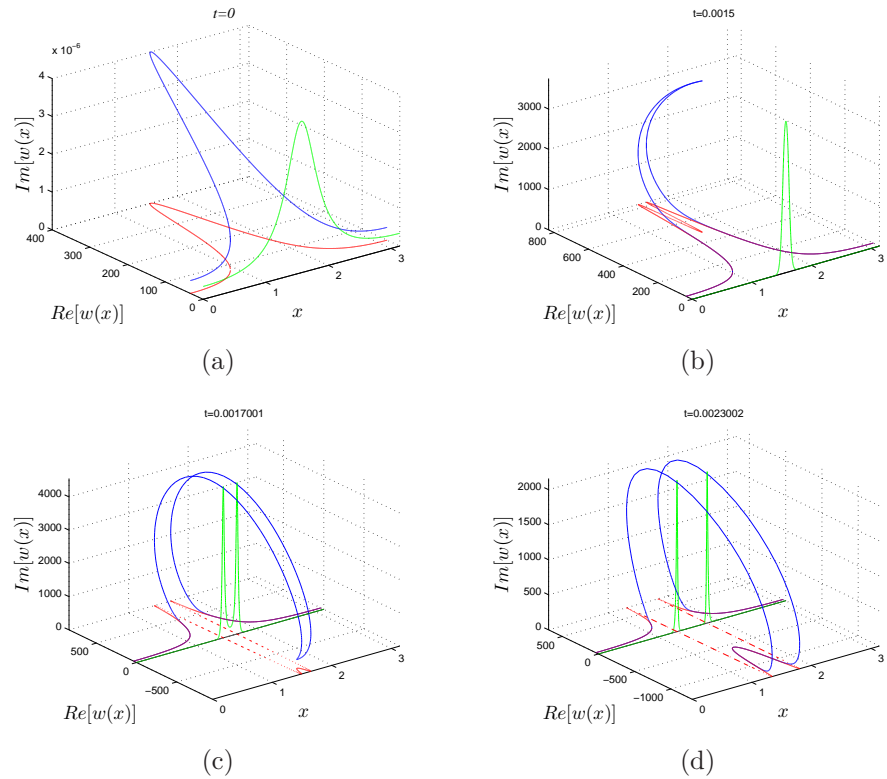


**Figure 4.** (Color online) The figure shows the solution of the complex equation associated with the real and imaginary parts of Eqs. (27)-(28) at various time instances (a)  $t = 0$ , (b) just before the collapse time, where the complex solution starts “going back on itself” rather than collapse (as it would for purely real initial data), (c), (d) Snapshots of the solution “reemerging” on the other side (the negative real axis end of the complex plane). Notice the visual similarity with the images in Fig. 2. The link to a computational movie of this evolution can be found at <https://www.dropbox.com/s/rxeKr7umxa5b3ko/complexdynamics.avi?dl=0>

Our computational findings were complemented by a compactification approach, supporting the argument that infinity can be addressed in the same way as a regular point or a regular level set along the orbit. At the same time, a complexification of the model was observed to provide a regularization of the original real dynamics, avoiding the collapse of the latter and offering insight on how collapsing orbits can be envisioned as limiting scenarios of nonlinear dynamical systems within the complex plane.

Naturally, there are numerous directions of interest for potential future studies. Clearly, exploring additional examples and examining whether the ideas can be equally successfully applied to them is of particular relevance. In the context of ODEs, this is especially relevant as regards vector/multi-dimensional systems. A related, especially important part in the realm of ODEs is that of convergence of algorithms e.g. to fixed points (or extremizers) of functions. Recall that in such cases, a concern always is whether the code may diverge along the way, rather than reach a root (or an extremum). Our approach can be used to devise algorithms with the ability to systematically bypass infinities during the algorithmic iterations- and such a “boosted” algorithm may be useful towards achieving enhanced, possibly global convergence to the roots (or extrema) of a function. This is particularly interesting now that continuous time versions of time-honored discrete algorithms like Newton or Nesterov

iteration schemes have become a research focus; see the related discussions in [30–32].

On the PDE side, we are envisioning (and currently starting to explore) a multitude of emerging aspects. For instance, when a distributed waveform reaches infinity at a single point in space-time, different post-collapse outcomes are possible. For example, an alternative possibility to the infinity-crossing presented here has been argued to be that the solution may "depart" from infinity without crossing (the transient blowup in [21]), as in the case of the standard collapsing NLS equation discussed extensively in textbooks [5,6]. There, the crossing through infinity is precluded by the existence of conservation laws. Past the initial point, it is argued in [6,17] that the solution will return from infinity incurring a "loss of phase". At the bifurcation level, the work of [20] offers a suggestion of how the return from infinity manifests itself: there, a solution with a positive growth rate was identified, that was dynamically approached during the collapse stage. Yet a partial "mirror image" of that, with negative growth rate, which presumably is followed past the collapse point in order to return from infinity was also identified; see, in particular, Fig. 1 and especially Fig. 2 of [20].

It is also possible that such a "touch and return" from infinity may occur without the loss of phase as, e.g., in the recent work of [33]. In examining a nonlocal variant of NLS (motivated by  $\mathcal{PT}$ -symmetric considerations, i.e., systems invariant under the action of parity and time-reversal), Ref. [33] identified a solution that goes to infinity in finite time that can be theoretically calculated; subsequently this solution returns from infinity and then revisits infinity again, in a periodic way, always solely touching it and never crossing. This solution is analytically available in Eq. (22) of [33] and the collapse times are given by Eq. (23) therein; perhaps even more remarkably, the model itself is integrable. In this case, infinity is reached, subsequently returned from and then periodically revisited. Such an observation would arise in our context if the "original" PDE for  $u$  (i.e., a variant of Eq. (20)) had a spatiotemporal limit cycle that attained somewhere in space an extremal value  $r$ . Then,  $w(x,t) \equiv \frac{1}{u(x,t)-r}$  would feature the above phenomenology. Such cases where infinity is reached but not crossed merit separate examination. The same is true for solutions exhibiting entire intervals at infinity, whose support progressively grows (or anyway remains finite), bordered by moving "fronts"; here one may envision that the "good" equation develops compacton-like solutions [22].

A related issue that may be worth exploring with such techniques is the possibility of bursting mechanisms (e.g. [34,35] involving heteroclinic connections with entire invariant planes at infinity) and the associated emergence of extreme events in nonlinear PDEs. Generalizations of the techniques developed herein to settings where, rather than  $u(x,t), u_x(x,t) \rightarrow \infty$  (or this happens for other quantities associated with the dependent variable), as is, e.g., the case during the formation of shocks, should also be interesting to explore. Effectively, our considerations here can be thought of as identifying and numerically evolving the infinity level set of the solution. Thus, a related interesting direction for future work could be to try to connect the considerations herein with ones of level set methods [36,37], adapting the latter towards capturing, e.g., the regions of the singular buffers.

Equally relevant are explicit examples similar to the one herein where multiple collapses may occur and propagate. An intriguing such case is the *defocusing* scenario of the nonlinear Schrödinger equation,

$$iu_t = u_{xx} - 2|u|^2u \quad (29)$$

which, in fact, has been shown in [38] to possess solutions such as  $u(x,t) = 1/x$ , or

$$u(x,t) = \frac{2x(x^2 + 6it)}{x^4 - 12t^2} \quad (30)$$

with propagating singularities at  $x = \pm 12^{1/4}t^{1/2}$ , and

$$u(x, t) = \frac{3(x^8 + 16itx^6 - 120t^2x^4 + 720t^4)}{x(x^8 - 72t^2x^4 - 2160t^4)}. \quad (31)$$

It is obvious that to follow such dynamical examples, a methodology bearing features such as the ones discussed above is needed in order to bypass the continuously propagating singular points. In turn, generalizing such notions to higher dimensions (e.g., a two-dimensional variant of the analytically tractable example herein) and addressing collapsing waveforms both at points, as well as in more complex geometric examples such as curves [39] is of particular interest for future studies.

It is tempting to explore whether the tools developed here may have something to add in the way we analyze collapse in well-established PDEs like the Navier-Stokes, or even singularities arising in a cosmological context. Several of these topics are under active consideration and we hope we will be able to report on them in future publications.

## Appendix

### Parabola Self-Similar Crossing

In the 1d case, starting from the assumption of a self-similar solution approaching infinity, we can prescribe a generic “unimodal” profile of the form:

$$u \sim \frac{1}{(t^* - t)^a} f\left(\frac{x - x_0}{(t^* - t)^b}\right), \quad (32)$$

where  $t^*$  is the collapse time and  $x_0$  is the point around which the blowup solution is centered.

Then, around  $x = x_0$  (and for  $t \neq t^*$ ), we can use a Taylor expansion locally in the form:

$$u \sim \frac{1}{(t^* - t)^a} \left[ f(0) + f'(0) \frac{x - x_0}{(t^* - t)^b} + \frac{f''(0)}{2} \frac{(x - x_0)^2}{(t^* - t)^{2b}} \right] \quad (33)$$

Combining the powers and bringing the dominant power to the left, we obtain that the field  $v$ , defined as

$$v \equiv u(t^* - t)^{a+2b} \sim \left[ f(0)(t^* - t)^{2b} + \frac{f''(0)}{2}(x - x_0)^2 \right], \quad (34)$$

behaves like a “regular” field which crosses  $v = 0$  at  $x = x_0$ , when  $t = t^*$ . So, its dynamics should be that of a “rising parabola”, cutting through 0 at the critical time. In Eq. (34), we also used the fact that  $x = x_0$  was an extremum (having in mind in particular a maximum) of the profile of the solution (hence  $f'(0) = 0$ ).

### MN-Dynamics

As an auxiliary tool in our analysis, we will outline here and utilize the so-called MN-dynamics [28], i.e., the self-similar dynamical evolution of a PDE which is collapsing towards a dynamical formation of a singularity. This approach has been used in porous medium type equations, as well as in dispersive (and conservative) NLS equations [20] and is broadly applicable to problems with self-similar growth (or decay). To illustrate it in a general form, we consider an evolutionary PDE of the form:

$$u_t = \mathcal{L}[\partial_\xi]u + \mathcal{N}[u], \quad (35)$$

By  $\mathcal{L}$  here we designate the operator involving derivatives (not necessarily a linear operator – see also the example below), while by  $\mathbf{N}$  we designate the local nonlinearity bearing operator.

Using the ansatz

$$u = A(\tau)f(\xi, \tau); \quad \xi = \frac{x}{L(\tau)}, \quad \tau = \tau(t) \quad (36)$$

we introduce a new scaled system of coordinates, intended to be suitably adjusted to the self-similar variation of the PDE solution.  $\xi$  is a rescaled spatial variable (taking into consideration the shrinkage –or growth– of the width), while  $\tau$  is a rescaled time variable, not a priori tuned, but which will be adjusted so that in this “co-exploding” frame, we factor out the self-similarity, in the same way in which when going to the co-traveling frame, we factor out translation. This way, the self-similar solution resulting in this dynamical frame will appear to be steady. Direct substitution of Eq. (36) inside of Eq. (35) yields:

$$\left[ A_\tau f + A f_\tau - A \xi f_\xi \frac{L_\tau}{L} \right] \tau_t = \mathcal{L}[\partial_\xi] f \frac{A}{L^a} + A^s \mathcal{N}[f] \quad (37)$$

where  $a$  and  $s$  are powers tailored to the particular problem (linear and nonlinear operators) of interest. In order to match the scalings of the two terms of the right hand side of Eq. (37), as is required for self-similarity, we demand that:

$$\frac{1}{L^a} = A^{s-1} \Rightarrow A \sim L^{-\frac{a}{s-1}} \Rightarrow G \equiv \frac{A_\tau}{A} = -\frac{a}{s-1} \frac{L_\tau}{L} \quad (38)$$

Thus, the model can now be rewritten as:

$$\left[ G \left( f + \frac{s-1}{a} \xi f_\xi \right) + f_\tau \right] \tau_t = A^{s-1} (\mathcal{L}[\partial_\xi] f + \mathcal{N}[f]). \quad (39)$$

Demanding then that the time transformation be such that there is evolution towards a stationary state in this co-exploding frame, we remove any explicit time dependence by necessitating that  $\tau_t = A^{s-1} \sim L^{-a}$ . Then, the stationary state in this frame will satisfy:

$$G \left( f + \frac{s-1}{a} \xi f_\xi \right) = \mathcal{L}[\partial_\xi] f + \mathcal{N}[f]. \quad (40)$$

It should be mentioned here that this analysis already provides an explicit estimate for the growth/shrinkage of amplitude and width over time, given that we assume that  $A_\tau/A = G = \text{const.}$  In particular,  $A_t = A_\tau \tau_t = A_\tau A^{s-1} = G A^s$ , which in accordance to the considerations of the previous section leads to the evolution of  $A \sim (t^* - t)^{1/(-s+1)}$ . A similar analysis can be performed for  $L$  such that  $L_t = L_\tau \tau_t = L_\tau L^{-a} = -G \frac{s-1}{a} L^{1-a}$ , leading to  $L \sim (t^* - t)^{\frac{1}{a}}$ . As a result of this analysis, our pulse-like entity touching (and potentially) crossing infinity will do so in a self-similar manner.

For the specific example of Eq. (21), using  $w = Af(\xi, \tau)$ , we obtain that

$$\mathcal{L}[\partial_\xi] w = \frac{A}{L^2} (w_{\xi\xi} - \frac{2}{w} w_\xi^2); \quad \mathcal{N}[w] = Aw + A^2 w^2 \quad (41)$$

It is then evident that the dynamics is not directly self-similar (due to the different scaling of the two terms within  $\mathcal{N}$ ), but only *asymptotically self-similar*. When  $w$  (and  $A$ ) is small, the exponential growth associated with the linear term is dominant.



However, as the amplitude increases, eventually the quadratic term takes over, leaving the linear term as one of ever-decreasing-significance “offending” to the exact self-similar evolution. When the linear term becomes negligible, the self-similar evolution requires that  $A/L^2 = A^2$ , providing the scaling of  $A \sim 1/L^2$ , i.e., in this case  $s = 2$  and  $a = 2$  for the general formulation above. From there, all the scalings associated with self-similarity can be directly deduced as explained previously.

## Supporting Information

### The linear ODE case

The mapping of the dynamics onto a circle can also be performed for the case of the simple exponential (rather than the power law self-similar, finite-time collapse) arising from the simple linear ODE of the form:

$$\dot{x} = \pm x. \quad (42)$$

with the standard solution

$$x(t) = e^{\pm(t-t^*)}. \quad (43)$$

Here the dynamics can be written in hyperbolic form as

$$\left(\frac{e^{\mp(t-t^*)} + x}{2}\right)^2 - \left(\frac{e^{\mp(t-t^*)} - x}{2}\right)^2 = 1, \quad (44)$$

and the variables

$$X = \cos(\theta) = \frac{e^{\pm(t^*-t)} - x}{e^{\pm(t^*-t)} + x} \quad (45)$$

$$Y = \sin(\theta) = \frac{2}{e^{\pm(t^*-t)} + x}, \quad (46)$$

can be defined so that  $X^2 + Y^2 = 1$ . In fact, substituting the exact solution of Eq. (43), it is straightforward to realize that  $X = \tanh(\mp(t - t^*))$  and  $Y = \operatorname{sech}(t - t^*)$ , resulting in the circular dynamics being a realization of the simple identity  $\tanh^2 + \operatorname{sech}^2 = 1$ .

### An asymptotically self-similar ODE case

We so far focused on genuinely self-similar examples; the corresponding ideas can also be extended to *asymptotically* self-similar cases [1] that are not genuinely self-similar in that they possess “offending” terms, yet upon approaching the singularity the self-similar terms dominate, with the offending ones playing a progressively less important role. Our approach can easily be adapted to this case.

Our simple example variant here will be of the form:

$$\dot{x} = 2x + x^2. \quad (47)$$

Direct integration again can yield the exact solution in the form:

$$x(t) = \frac{2e^{2(t-t^*)}}{1 - e^{2(t-t^*)}}. \quad (48)$$

It can be seen (when integrating Eq. (47)) that in this case the observable  $\log(x/(x+2))$  is the one that linearly crosses through 0 (as  $2(t-t^*)$ ). For  $x$  large, this quantity becomes

$$\log\left(\frac{1}{1 + \frac{2}{x}}\right) \approx -2\frac{1}{x} + 2\frac{1}{x^2} - \frac{8}{3}\frac{1}{x^3} \quad (49)$$

Hence, indeed at large times, it is the quadratic term that takes over since the dominant behavior of  $x(t)$  is like  $1/(t^* - t)$ . However, as  $t \rightarrow t^*$ , the relevant asymptotics reads:

$$x(t) = \frac{1}{t^* - t} - 1 + \frac{t^* - t}{3} - \frac{(t^* - t)^3}{45} + \dots \quad (50)$$

enabling one to observe the explicit (lower order) contribution of the terms offending to the self-similarity. the collapse time, denoted by  $t^*$ , is still determined by the initial data as  $t^* = -(1/2) \log(x(0)/(x(0) + 2))$ .

Nevertheless, in this case as well, our computational prescription can be carried out. Eq. (47) can be integrated until  $x$  becomes large. we then revert to  $y = 1/x$  which has the straightforward ODE dynamics:

$$\frac{dy}{dt} = -2y - 1 \quad (51)$$

(using the transformation to obtain the initial condition  $y(0)$ ) and the equally simple solution  $y(t) = -1/2 + (y(0) + 1/2)e^{-2t}$ . The solution of the latter problem of Eq (51) crosses 0 en route to its approach of the asymptotic value of  $-1/2$ . Finally, once the infinity has been bypassed, we return to the simulation of Eq. (47), as before.

*Mapping the dynamics to a circle.* The solution of Eq. (47) can be rewritten as:

$$x(t) = \frac{2}{e^{2(t^*-t)} - 1} \Rightarrow x \frac{(e^{2(t^*-t)} - 1)}{2} = 1. \quad (52)$$

Using the compactification the exact same way as Eqs. [3] and [4] of the main text and only replacing  $t^* - t$  with:  $(e^{2(t^*-t)} - 1)/2$ , the compactification scheme carries through.

a) In this case, if  $t \rightarrow t^*$ , we Taylor expand and retrieve (from the first term) the limit of exactly Eqs. [3]–[4]. This is the contribution that stems from the  $x^2$  term in the ODE.

b) In the case of  $t \rightarrow 0$  (or anyway far from  $t^*$ ) the exponential dominates and the (-1) coming from the  $x^2$  term is irrelevant. This is the contribution that stems from the  $2x$  term in the ODE.

## Time to transition

Following numerous works including [26, 27], we consider a radial contour along the complex plane i.e., the arc of a circle from the real to the positive imaginary axis. Then, along this arc (denoted by  $C$ ), we have for  $T$ , the elapsed time:

$$T = \int_C dt = \int_C \frac{dz}{z^3} = \int_0^{\pi/2} \frac{Rie^{i\phi}}{R^3 e^{3i\phi}} d\phi. \quad (53)$$

Bearing in mind the radial nature of the contour (which renders  $R$  constant), factoring out  $1/R^2$  and taking the limit as  $R \rightarrow \infty$ , we obtain a vanishing result, even though the angular integral amounts to unity. I.e., interestingly, it takes a finite time to reach from everywhere along the real axis an equidistant point along the imaginary axis, yet this time vanishes as we approach infinity, in line with the analytical result for  $\dot{x} = x^3$ . In the case of  $\dot{z} = z^2$ , there is a similar result justifying the infinitesimal time of return there from the positive to the negative real axis.

---

## Acknowledgments

The authors gratefully acknowledge support from the US NSF and the US Air Force Office of Scientific Research (Dr. F. Darema), as well as stimulating discussions with Profs. D. Aronson, C. Bender, E. Bollt, P. Constantin, M. Dafermos, C. Tully and Z. Musslimani.

## References

1. G.I. Barenblatt, *Scaling*, Cambridge University Press (Cambridge, 2003).
2. N. D. Goldenfeld. *Lectures on Phase Transitions and the Renormalisation Group*, Addison-Wesley (Boston, 1992).
3. J. Bona, V.A. Dougalis, O.A. Karakashian and W.R. McKinney Appl. Numerical Math. **10**, 335 (1992); see also J.L. Bona, V.A. Dougalis, O.A. Karakashian and W.R. McKinney, pp. 17–29 in Contemporary Math. **200**, F. Dias, J.-M. Ghidaglia & J.-C. Saut Eds. AMS (Providence, 1996).
4. G. Fibich and G.C. Papanicolaou, SIAM J. Appl. Math. **60**, 183 (1999).
5. C. Sulem and P.L. Sulem, *The Nonlinear Schrödinger Equation*, Springer-Verlag (New York, 1999).
6. G. Fibich, *The Nonlinear Schrödinger Equation*, Springer-Verlag (Heidelberg, 2015).
7. D. Slepcev and M.C. Pugh, Indiana Univ. Math. J. **54**, 1697 (2005); T.P. Witelski, A.J. Bernoff and A.L. Bertozzi, European J. Appl. Math. **15**, 223 (2004).
8. S.B. Angenent and D.G. Aronson, European J. Appl. Math. **7**, 277 (1996); D.G. Aronson, Discr. Cont. Dyn. Sys. **17**, 1685 (2012).
9. J.M. Foster, D.E. Pelinovsky, *Self-similar solutions for reversing interfaces in the nonlinear diffusion equation with constant absorption*, preprint available at: <http://dmpeli.math.mcmaster.ca/>
10. R.V. Kohn and X. Yan, Comm. Pure App. Math. **56**, 1549 (2003).
11. O. Morsch and M. Oberthaler, Rev. Mod. Phys. **78**, 179 (2006).
12. Y.V Kartashov, B.A. Malomed, L. Torner, Rev. Mod. Phys. **83**, 247 (2011).
13. M. Olshanii, S. Choi, V. Dunjko, A.E. Feiguin, H. Perrin, J. Ruhl, D. Aveline, Phys. Lett. A **380**, 177 (2016).
14. H. Saito and M. Ueda Phys. Rev. Lett. **90**, 040403 (2003).
15. M. Centurion, M.A. Porter, P. G. Kevrekidis, and D. Psaltis Phys. Rev. Lett. **97**, 033903 (2006).
16. S. Tzortzakis, L. Bergé, A. Couairon, M. Franco, B. Prade, and A. Mysyrowicz Phys. Rev. Lett. **86**, 5470 (2001).
17. B. Shim, S.E. Schrauth, A.L. Gaeta, M. Klein, and G. Fibich Phys. Rev. Lett. **108**, 043902 (2012)

- 
18. W Ren, XP Wang *J. Comp. Phys* **159**, 246 (2000).
  19. W. Huang and R.D. Russell, *Adaptive Moving Mesh Methods*, Springer-Verlag (New York, 2011).
  20. C.I. Siettos, I.G. Kevrekidis and P.G. Kevrekidis, *Nonlinearity* **16**, 497 (2003).
  21. V.A. Galaktionov, J.L. Vásquez, *Discr. Cont. Dyn. Sys.* **8**, 399 (2002).
  22. P. Rosenau and J.M. Hyman *Phys. Rev. Lett.* **70**, 564 (1993).
  23. <http://www.math.uoc.gr/~pamfilos/eGallery/problems/HyperbolaGeneration.html>
  24. I.G. Kevrekidis, B. Nicolaenko, J.C. Scovel, *SIAM J. Appl. Math.* **50**, 760 (1990).
  25. [http://www.scholarpedia.org/article/Heteroclinic\\_cycles](http://www.scholarpedia.org/article/Heteroclinic_cycles)
  26. E. Fontich, J. Sardanyés, *J. Phys. A. Math. Theor* **41**, 015102 (2008).
  27. C.M. Bender, D. C. Brody, D.W. Hook, *J. Phys. A Math. Theor* **41**, 352003 (2008).
  28. D.G. Aronson, S.I. Betelu, I.G. Kevrekidis [arXiv:nlin/0111055](https://arxiv.org/abs/nlin/0111055).
  29. C.N. Dawson, Q. Du and T.F. Dupont. *Math. Comp.* **57**, 63 (1991).
  30. P.E. Farrell, A. Birkisson, S.W. Funke, [arXiv:1410.5620](https://arxiv.org/abs/1410.5620).
  31. W. Su, S. Boyd, E.J. Candés, [arXiv:1503.01243](https://arxiv.org/abs/1503.01243).
  32. A. Wibisono, A.C. Wilson, M.I. Jordan, [arXiv:1603.04245](https://arxiv.org/abs/1603.04245).
  33. M.J. Ablowitz and Z.H. Musslimani, *Phys. Rev. Lett.* **110**, 064105 (2013).
  34. J. Moehlis, E. Knobloch, *Phys. Rev. Lett.* **80**, 5329 (1998).
  35. E. Knobloch and J. Moehlis, in "Pattern Formation in Continuous and Coupled Systems", M. Golubitsky, D. Luss and S.H. Strogatz (Eds.) Springer-Verlag (Berlin, 1999), pp. 157.
  36. J.A. Sethian, "Level Set Methods; Evolving Interfaces in Geometry, Fluid Mechanics, Computer Vision and Material Sciences", Cambridge University Press (Cambridge, 1996).
  37. J.A. Sethian and P. Smereka, *Ann. Rev. Fluid Mech.* **35**, 341, (2003).
  38. P.A. Clarkson, *European J. Appl. Math.* **17**, 293 (2006).
  39. G. Baruch, G. Fibich, N. Gavish, *Physica D* **239**, 1968 (2010).